

T Pyxidis: death by a thousand novae

Joseph Patterson,¹★† Arto Oksanen,² Jonathan Kemp,³† Berto Monard,⁴ Robert Rea,⁵ Franz-Josef Hambsch,⁶ Jennie McCormick,⁷ Peter Nelson,⁸ William Allen,⁹ Thomas Krajci,¹⁰ Simon Lowther,¹¹ Shawn Dvorak,¹² Jordan Borgman,¹ Thomas Richards,¹³ Gordon Myers,¹⁴ Caisey Harlinton¹⁵ and Greg Bolt¹⁶

¹Department of Astronomy, Columbia University, 550 West 120th Street, New York, NY 10027, USA

²CBA–Finland, Hankasalmi Observatory, Verkkoniementie 30, FI-40950 Muurame, Finland

³Department of Physics, Middlebury College, Middlebury, VT 05753, USA

⁴CBA–Kleinkaroo, Klein Karoo Observatory, PO Box 281, Calitzdorp 6660, South Africa

⁵CBA–Nelson, Regent Lane Observatory, 8 Regent Lane, Richmond, Nelson 7020, New Zealand

⁶CBA–Mol, Andromeda Observatory, Oude Bleken 12, B-2400 Mol, Belgium

⁷CBA–Pakuranga, Farm Cove Observatory, 2/24 Rapallo Place, Farm Cove, Pakuranga, Auckland 2012, New Zealand

⁸CBA–Victoria, Ellinbank Observatory, 1105 Hazeldean Road, Ellinbank, VIC 3821, Australia

⁹CBA–Blenheim, Vintage Lane Observatory, 83 Vintage Lane, RD 3, Blenheim 7273, New Zealand

¹⁰CBA–New Mexico, PO Box 1351 Cloudcroft, NM 88317, USA

¹¹CBA–Pukekohe, Jim Lowther Observatory, 19 Cape Vista Crescent, Pukekohe 2120, New Zealand

¹²CBA–Orlando, Rolling Hills Observatory, 1643 Nightfall Drive, Clermont, FL 34711, USA

¹³CBA–Melbourne, Pretty Hill Observatory, PO Box 323, Kangaroo Ground, VIC 3097, Australia

¹⁴CBA–San Mateo, 5 Inverness Way, Hillsborough, CA 94010, USA

¹⁵Caisey Harlinton Observatory, The Grange, Scarrow Beck Road, Erpingham, Norfolk NR11 7QX, UK

¹⁶CBA–Perth, 295 Camberwarra Drive, Craigie, WA 6025, Australia

Accepted 2016 November 15. Received 2016 November 14; in original form 2016 February 29

ABSTRACT

We report a 20-yr campaign to track the 1.8 h photometric (and orbital) wave in the recurrent nova T Pyxidis. Before and after the 2011 eruption, the period increased on a time-scale $P/\dot{P} = 3 \times 10^5$ yr. This suggests a mass transfer rate in quiescence of $\sim 10^{-7} M_{\odot} \text{ yr}^{-1}$, in substantial agreement with the *accretion* rate based on the star's luminosity. During the eruption itself, a rapid period increase of 0.0054(7) per cent occurred. This is probably a measure of the mass ejected in the outburst. For a plausible choice of binary parameters, that mass is at least $3 \times 10^{-5} M_{\odot}$, and probably more. This represents >300 yr of accretion at the pre-outburst rate, but the time between outbursts was only 45 yr. Thus, the erupting white dwarf (WD) seems to have ejected at least six times more mass than it accreted. If this eruption is typical, the WD must be eroding, rather than growing, in mass. Unless the present series of eruptions is a short-lived episode, the binary dynamics will evaporate the secondary in $\sim 10^5$ yr. This could be a major channel by which short-period cataclysmic variables are removed from the population.

Key words: accretion, accretion discs – binaries: close – stars: individual: T Pyxidis – novae, cataclysmic variables.

1 INTRODUCTION

T Pyxidis (T Pyx) is the Galaxy's most famous recurrent nova. Six times since 1890, the star has erupted to $V = 6$, and then subsided

back to quiescence near $V = 15$. With spectroscopy and detailed light curves known for several of these eruptions, and with a fairly bright quiescent counterpart, T Pyx has become a well-studied star – sometimes considered a prototype for recurrent novae. Selvelli et al. (2008) and Schaefer, Pagnotta & Shara (2010, hereafter SPS) give recent reviews, and the 2011 eruption has propelled the star back into the journals with gusto (Schaefer et al. 2013; Shore et al. 2013; Chomiuk et al. 2014; Nelson et al. 2014).

Since they are believed (and in a few cases known) to possess massive white dwarfs (WDs) accreting at a high rate, recurrent novae are a promising source for Type Ia supernovae. As they

* E-mail: jop@astro.columbia.edu

† Visiting Astronomer, Cerro Tololo Inter-American Observatory, National Optical Astronomy Observatories which is operated by the Association of Universities for Research in Astronomy, Inc., (AURA) under cooperative agreement with the National Science Foundation.

also *eject* matter, their candidacy rests on the assumption that mass accretion in quiescence exceeds mass ejection in outburst. Estimates of these rates are notoriously uncertain, and that assumption has never undergone a significant test. A *dynamical* measure of the mass ejected, based on the precise orbital period change in outburst, would furnish the most precise and compelling evidence.

In the late 1980s, it was recognized that T Pyx might soon furnish that information, since an outburst could occur soon (optimists suggested 1988, based on the 1966 outburst and the estimated 22-yr mean interval). However, the orbital period was not yet known; several photometric and spectroscopic studies gave discrepant periods, and all are now known to be incorrect.¹

Schaefer et al. (1992) identified a persistent photometric wave with a period of 0.076 d, but discounted that as a possible orbital period, since it was not coherent from night to night. They interpreted it as a ‘superhump’ – arising from precession of the accretion disc – and estimated an underlying P_{orb} near 0.073 d. A 1996–1997 observing campaign (Patterson et al. 1998, hereafter P98) revealed that the weak 0.076 d signal, difficult to discern over a single cycle, is actually quite coherent, maintaining a constant phase and amplitude over many thousands of cycles. With a precise ephemeris, it bears all the earmarks of a bona fide orbital period. Remarkably, that study of all timings during 1986–1997 revealed an enormous rate of period increase, with $P/\dot{P} = 3 \times 10^5$ yr. Any remaining dissent from the P98 orbital-period interpretation fell away when Uthas, Knigge & Steeghs (2010, hereafter UKS) found radial-velocity variations precisely following the 0.07622 d period, but only when the same increasing-period photometric ephemeris was adopted (see their fig. 2).

This paper reports on our long-term photometric study of T Pyx with the globally distributed telescopes of the Center for Backyard Astrophysics (CBA). All the ‘quiescent’ data are basically consistent with the P98 ephemeris (slightly tweaked). And, as hoped, the signal returned after the 2011 eruption – with a different period. Thus, the sought after dynamical measure of ejected mass may have been achieved. We then revisit the P98 interpretation, educated by the 2011 eruption and the many recent studies of this amazing star.

2 OBSERVATIONS

Nearly all our observations are time-series differential photometry with the worldwide CBA telescopes (Skillman & Patterson 1993; Patterson et al. 2013, hereafter P13). Since our telescopes are small and the primary objective is detection and definition of periodic signals, most of the time series are obtained in unfiltered (white) light, to achieve high time resolution with good signal to noise. When we have many separate time series from different observatories, we use their overlaps to measure additive constants and thereby splice the data to obtain a longer time series on a common (instrumentally defined) magnitude scale. Somewhat more commonly, the various time series do not overlap, in which case we usually subtract the mean and trend to obtain a ‘zeroed’ file. By merging all the zeroed files, we then obtain a long time series with zero mean. This latter approach artificially blinds us to very low frequencies (below ~ 3

cycles per day²), but is optimum for the study of higher frequencies that are our usual targets for analysis.

A summary log of observations is given in Table 1, where we have included the P98 data for completeness. Each ‘night’ consists of a time series from one observer – and hence there is occasional redundancy that helps us with calibration among observatories. During quiescence, at least 24-h of observation were obtained during each season (except 2010), in order to accurately track any changes in period or waveform in the 0.07623 d orbital signal. During and after the 2011 outburst, we increased the coverage substantially. The total was 2002 h of photometry on 497 nights during 1996–2016.

Light curves on single nights during quiescence are usually dominated by erratic flickering, illustrated by fig. 8 of P98. For each cluster of data with dense spacing, we calculated the power spectrum, found a signal at the orbital period P_{orb} , and then folded on P_{orb} to obtain the mean orbital light curve. These waveforms were slightly variable but always contained a distinct dip of ~ 0.08 mag full amplitude. Some of these waveforms will be shown below. Presumably because of flickering, we found that at least 7–10 orbits were needed to obtain a stable waveform.

The periodic signal became much weaker in outburst, and we used much longer data streams (20–50 orbits) to search for the periodic signal. It did not appear clearly until day 170 of the eruption, and then increased in strength as the star faded. More details will be presented in Section 4.

3 PRE-OUTBURST (1996–2011)

Following the report of a 1.8 h quasi-period by S92, we made T Pyx a priority target for time-series photometry. In the 1996–1997 campaign, we proved the existence of a strict 0.07623 d period, stable in phase and waveform over a 1-yr baseline – and deduced a long-term cycle count that tied together timings of minima over the full 1986–1997 baseline (P98). Some doubt still remained about this cycle count; it relied on quite sparse timings earlier than 1996, and also required hypothesizing a rate of (orbital?) period change that was orders of magnitude greater than anything previously seen in cataclysmic variables.

Great stability is the main credential certifying an orbital origin, and we studied the light curves for stability and timing during each observing season since 1996. By 1999, it was clear that the P98 ephemeris was confirmed. Averaged over each dense cluster of photometry during each season, the 1.8 h signal was stable in period, amplitude, and phase. The waveform was always close to that of fig. 10 in P98, and the timings of primary minimum tracked the P98 ephemeris, thus verifying the cycle count and the signal’s consequent high stability and high \dot{P} . The 1996–2009 CBA increasing-period photometric ephemeris was the basis of the successful phase-up of radial velocities by UKS (their fig. 2).

Those timings of 1996–2011 minima, each averaged over 5–15 orbits, are reported in Table 2, and reduced to an O–C diagram in Fig. 1. The upward curve indicates a steadily increasing period, and the good fit of the parabola is consistent with a constant rate of

¹ For the record, these periods are 0.1433 d (Barrera & Vogt 1989), 0.1100 or 0.0991 d (Schaefer 1990), and ~ 0.073 d (Schaefer et al. 1992, hereafter S92).

² In this paper, we routinely use cycles per day, or cycles d^{-1} , as the unit of frequency. ‘Day’ is the natural unit of time in a long series of night-time observation, and cycles per day is our natural unit of frequency, since daily aliases are a great hazard in studies of periodic signals from our rotating planet.

Table 1. Summary log of observations.

<i>Year</i>	<i>Nights/hours</i>	<i>Observers</i>
1995–1996	14/85	Patterson
1996–1997	7/29	Patterson
1997–1998	8/33	Kemp
1998–1999	8/29	Kemp
1999–2000	6/26	Kemp
2000–2001	5/24	McCormick
2001–2002	4/24	Kemp, McCormick
2002–2003	19/71	Rea, Kemp, Monard, Allen, Richards
2003–2004	10/39	Rea, Allen, Monard
2004–2005	7/24	Rea, Monard, McCormick
2005–2006	23/90	Allen, Rea, Monard, Christie, McCormick
2006–2007	30/99	McCormick, Allen, Monard, Bolt
2007–2008	18/74	Rea, Bolt
2008–2009	15/62	Rea, Monard, McCormick, Bolt
2010–2011	7/24	Rea, Myers (before eruption)
2011	102/400	Oksanen, Harlinton, Monard, Lowther, Dvorak, Bolt, Krajci, Hamsch (eruption)
2011–2012	54/221	Oksanen, Harlinton, Monard, Hamsch, Myers
2012–2013	68/243	Oksanen, Monard, Nelson, Hamsch, McCormick
2013–2014	15/61	Monard, Nelson, Oksanen, Myers
2014–2015	33/154	Myers, Oksanen, Monard, Dvorak, Hamsch
2015–2016	49/128	Nelson, Monard, Myers, Hamsch, Dvorak
<i>Observer</i>	<i>Telescope</i>	<i>Location/observatory</i>
Kemp	1.0 m/0.9 m	La Serena, Chile (CTIO)
Oksanen	0.5 m	San Pedro de Atacama, Chile (CaiseyHarlinton Observatory)
Allen	0.4 m	Nelson, New Zealand (Vintage Lane Observatory)
Rea	0.35 m	Nelson, New Zealand (Regent Land Observatory)
McCormick	0.35 m	Auckland, New Zealand (Farm Cove Observatory)
Monard	0.35 m	Calitzdorp, South Africa (Klein-Karoo Observatory)
Hamsch	0.4 m	San Pedro de Atacama, Chile (ROAD Observatory)
Nelson	0.3 m	Melbourne, Australia (Ellinbank Observatory)
Christie	0.4 m	Auckland, New Zealand (Auckland Observatory)
Bolt	0.35 m	Perth, Australia
Dvorak	0.3 m	Orlando, Florida, USA (Rolling Hills Observatory)
Patterson	1.0 m/0.7 m	La Serena, Chile (CTIO) / Sutherland, South Africa (SAAO)
Myers	0.42 m	Siding Spring, Australia
Richards	0.3 m	Melbourne, Australia (Pretty Hill Observatory)
Lowther	0.25 m	Pukekohe, New Zealand (Jim Lowther Observatory)
Krajci	0.35 m	Cloudcroft, New Mexico, USA

period change. The curve corresponds to the ephemeris

$$\text{Minimum} = \text{HJD } 2450124(1) + 0.0762263(2)E + 2.38(8) \times 10^{-11} E^2. \quad (1)$$

This implies $dP/dt = 6.4 \times 10^{-10}$, or $P/\dot{P} = 3.3 \times 10^5$ yr. This should be compared to P98’s fig. 12 that included also the much sparser 1986–1990 timings.

4 ERUPTION AND AFTERMATH

4.1 The long-awaited eruption

The outburst was discovered and announced by Michael Linnolt on 2011 April 14 (JD 2455666). We will refer to this as ‘day 0’ of the eruption, although subsequent archaeology showed a brightening that started a few days earlier. Schaefer et al. (2013, hereafter S13) provide a fascinating and detailed blow-by-blow account. We then obtained time-series photometry on ~300 of the next ~500 nights, totalling ~1100 h. We used the same techniques as at quiescence: segregate the data into dense clusters over ~4–10 nights, and look for periodic signals in each. Near maximum light, no periodic signals were found over the frequency range 3–1000 cycles per day.

The full (peak-to-trough) amplitude upper limit for signals near the orbital frequency was 3–4 mmag. For frequencies above 100 cycles d^{-1} , the upper limit was ~1 mmag.

The first obvious detection of a periodic signal occurred when the star emerged from solar conjunction, around day 180 ($V = 11$). A 12-night time series yielded a clear signal at the orbital frequency, with an amplitude of 4 mmag. This signal grew steadily in amplitude as the star continued its decline from maximum light. Two dense clusters near day 70 (when $V = 9$, prior to solar conjunction) also produced *likely* detections of ω_{orb} . These were not statistically significant in the power spectra, but synchronous summation at P_{orb} yielded the familiar waveform, and gave timings of minimum light consistent with the post-eruption ephemeris. Therefore, these detections should be considered likely but not certain.

4.2 Periodic signals, yes; aliasing, yes

After day 150, each segment showed a strong detection at ω_{orb} , a weaker detection at $2\omega_{\text{orb}}$, and no other significant and repeatable signals. A typical power spectrum is shown in the upper frame of Fig. 2, and is substantially identical to the power spectra of quiescence. For several segments, peaks near $\omega_{\text{orb}} - 3.00$ or $2\omega_{\text{orb}} + 3.00$ cycles per day were surprisingly strong, and we briefly considered

Table 2. Timings of orbital minima.

A. Pre-outburst ^d					
Minimum (HJD 2 450 000+)					
124.830	164.893	189.548	212.491	460.609	548.497
820.931	870.554	1171.804	1651.652	1930.872	2323.903
2624.9273	2658.9994	2718.9171	3055.3867	3396.9675	3738.0087
3751.1261	3770.9415	4113.2874	4144.9212	4152.3152	4178.9918
4467.0638	4481.9269	4852.9376	4913.9227	4939.3021	5560.9545
5588.9313	5598.9173				
B. Outburst and aftermath					
Minimum (HJD 2450 000+)	Amplitude (mag)	V	Minimum (HJD 2 450 000+)	Amplitude (mag)	V
5835.8433	0.005	11.35	5879.8317	0.005	11.76
5890.7328	0.006	11.96	5900.7192	0.008	12.11
5909.6416	0.014	12.28	5924.6566	0.011	12.41
5934.6436	0.012	12.57	6001.6534	0.025	13.40
6034.5868	0.019	13.66	6063.5504	0.028	13.86
6102.5077	0.037	14.06	6234.7755	0.054	14.82
6255.7385	0.073	14.86	6265.8025	0.058	14.86
6274.7963	0.071	14.90	6283.5640	0.078	15.05
6288.4432		15.07	6295.3809		15.10
6298.4277	0.069	15.08	6302.9992		15.11
6325.7200	0.070	15.10	6332.9637		15.12
6341.5781	0.072	15.12	6362.1625		15.18
6460.1963		15.31	6594.8262		15.44
6630.8065		15.46	6645.3680	0.073	15.52
6653.4510		15.54	6707.8808		15.58
6789.9121	0.077	15.57	6979.8113	0.075	15.62
7005.4227	0.080	15.70	7026.0085		15.71
7143.2512		15.70	7147.2185		15.71
7150.8799		15.68	7154.8431		15.68
7365.0971	0.080	15.81	7370.0501	0.081	15.85
7380.0412	0.096	15.84	7394.0682	0.090	15.85
7400.0104	0.073	15.83	7413.1240	0.072	15.74
7417.3196	0.074	15.73	7426.6939	0.076	15.79

Note. Consistent with $V = 15.6$, and amplitude 0.08 mag.

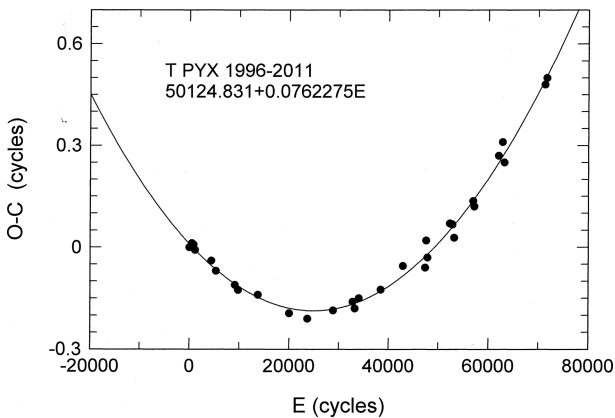


Figure 1. O–C diagram of the timings of primary minima during 1996–2011. The fit to a parabola indicates acceptable representation with a constant rate of period change ($P/\dot{P} = 3 \times 10^5$ yr).

whether these might be detections of an independent signal (for which P98 suggested weak evidence, and which has been sometimes interpreted as evidence for magnetically channelled accretion). However, subtraction of the orbital signal always weakened, and usually removed, this weaker signal. This is the sign of an alias. We show the analysis in the lower frames of Fig. 2. The spectral

window (power spectrum of a time series with a pure sinusoid at ω_{orb} artificially inserted) is shown in the middle frame; the close resemblance to the upper frame suggests that the sideband signals are entirely the result of sampling. As a second test, we subtracted the best-fitting sinusoid at ω_{orb} from the time series, and calculated the power spectrum of the residuals. This is shown in the lowest frame of Fig. 2. The power spectrum is pure noise, and the highest noise peak corresponds to a semi-amplitude of 0.0008 mag.

The power spectrum of Fig. 2 really was ‘typical’ (in its limitations, too). Because our programme attempted to follow the periodic signal over years, we made many observations at times when T Pyx was not optimally placed in the night sky – forcing us to splice many relatively short runs, and thus running a bigger risk of aliases. The corresponding result for one data segment obtained in February, when T Pyx transits near local midnight, is shown in Fig. 3. Here all the potential aliases are invisible, because the individual time series are long enough to bridge the longitude gaps in our network (the Atlantic, Pacific, and Indian Oceans).

4.3 Magnetism, probably no

We discuss this point at length because of the many previous papers that allege or cite evidence of *magnetism* in T Pyx. No such evidence, in the form of a photometric signal at a non-orbital frequency,

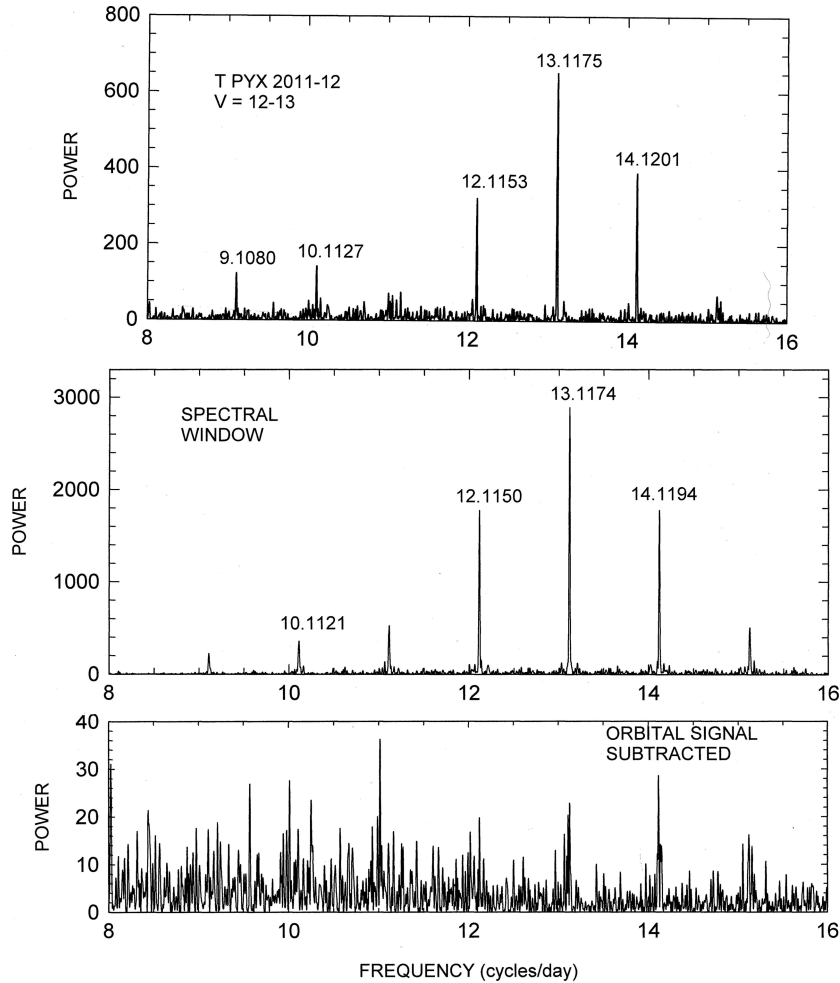


Figure 2. Upper frame: power spectrum of a 30-d segment of light curve soon after eruption. Signals are flagged with their frequency in cycles per day. The main signal at 13.1175 cycles d^{-1} appears strongly, and several likely aliases. Middle frame: power spectrum of an artificial time series, containing only the main signal and sampled exactly like the actual light curve. The close resemblance to the upper frame shows that the smaller peaks are entirely a result of aliasing. Lower frame: the power spectrum of the original time series after the main signal (period, amplitude, and phase) is subtracted, showing that no other signal is present, to a semi-amplitude upper limit of 0.6 mmag.

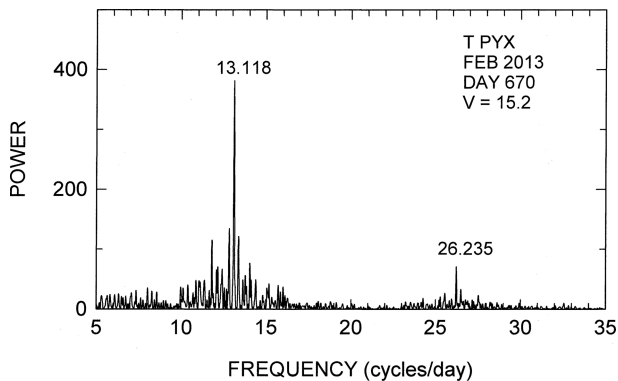


Figure 3. Power spectrum of a dense (20-d) segment of light curve, when the gaps between observing stations were minimal. The only significant signals are ω_{orb} and its harmonics; upper limits at other frequencies are typically ~ 4 mmag.

exists in our data. Some have also cited evidence from spectroscopy – namely the strong He II emission, sometimes thought to be associated with radial accretion. But He II emission is mainly indicative of high temperature, not the accretion geometry; and He II in T Pyx

appears to be of normal strength for very luminous CVs (see fig. 5 of Patterson & Raymond 1985, where T Pyx is the point at upper right). Photoionization by the disc’s boundary-layer radiation seems capable of powering He II emission of that strength ($\sim 5 \text{ \AA}$ equivalent width). The He II emission could also arise in a wind.

Of course, there could be magnetism lurking somewhere in the star – probably 20–30 per cent of all CVs show some magnetic effect (usually collimated accretion flow). But we know of no evidentiary basis for magnetism in T Pyx.³

4.4 Light curves, timings of minima, and period changes

For each segment, we folded the time series (~ 30 orbits near $V = 12\text{--}13$, and ~ 20 orbits near $V = 14\text{--}15.7$) on P_{orb} , and some of the mean light curves are shown in Fig. 4. The same general description applies: a roughly sinusoidal waveform, with a (relatively) large dip defining minimum light, and a small variable dip near maximum

³ But metaphorically, as everyone who studies T Pyx knows, the star is *hyper*-magnetic.

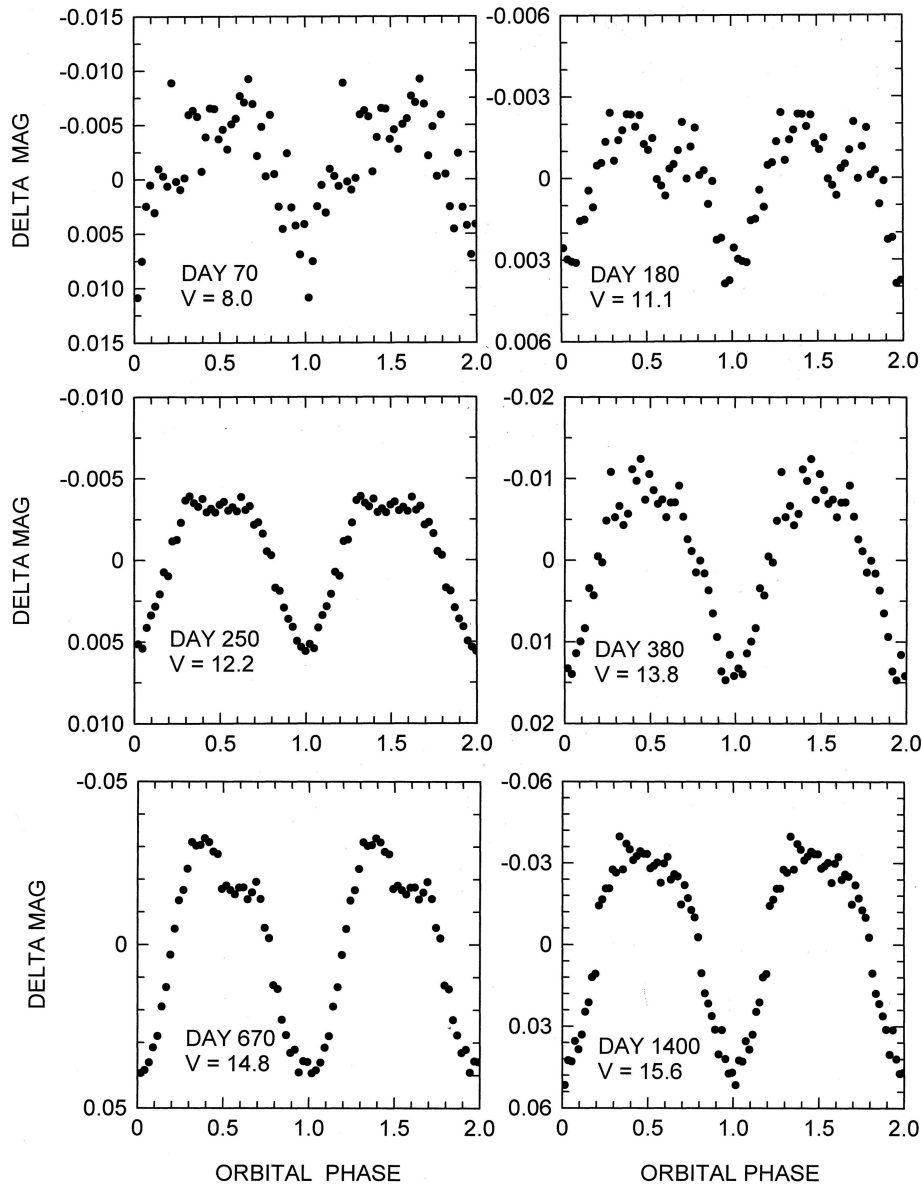


Figure 4. Orbital light curves at various points in the decline. Each is based on at least 20 orbits, and day numbers refer to the mid-point of the time series. The phase marker we have used – minimum light – appears to be stable within ~ 0.03 cycles. Despite appearances, the detection at day 70 is uncertain, since the peak in the power spectrum was too weak to be significant (this datum was obtained near the 2011 solar conjunction).

light. The waveforms are very similar to that of ‘pre-eruption quiescence’ (fig. 10 of P98). For each segment, we measured the average time of minimum light, along with the full amplitude of variation. The results are shown in Table 2. The best-fitting period just after eruption is 0.0762337(1) d, an increase over the period just prior to eruption by 0.0054(7) per cent. So large a period change is very, very surprising; it is seven times larger than the ΔP predicted by Livio (1991) – and of the opposite sign!

We also looked for period change after the eruption (2011.8–2016.1), from examining Fig. 5. This is an O–C diagram of the 42 timings with respect to a constant test period (0.076234 d). The upward curvature indicates a period increase, and the fitted parabola is equivalent to the elements

$$\begin{aligned} \text{Minimum} = & \text{HJD } 2456234.7753(4) + 0.07623361(6) E \\ & + 2.9(4) \times 10^{-11} E^2. \end{aligned} \quad (2)$$

The corresponding time-scale P/\dot{P} for period increase is then $2.4(4) \times 10^5$ yr – similar to the pre-outburst estimate in equation (1).

Unfortunately, O–C diagrams are no longer standard equipment in the astronomer’s toolbox. So, we show these effects more transparently in Fig. 6 that tracks period versus time during 1986–2016. Each period is a 2-yr running average; for example, the 2003 period is based on timings during 2002–2004. Fig. 6 shows the period increases before and after eruption, plus a very rapid increase that is roughly centred on the eruption (day 0 corresponding to year 2011.3).

The first two points in Fig. 6 are derived from the very sparse early timings collected in table 6 of P98. These are much less reliable, because they are mostly based on single-night light curves that ‘looked good’. Nevertheless, the cycle count established here is identical to the P98 cycle count, and the derived ephemerides

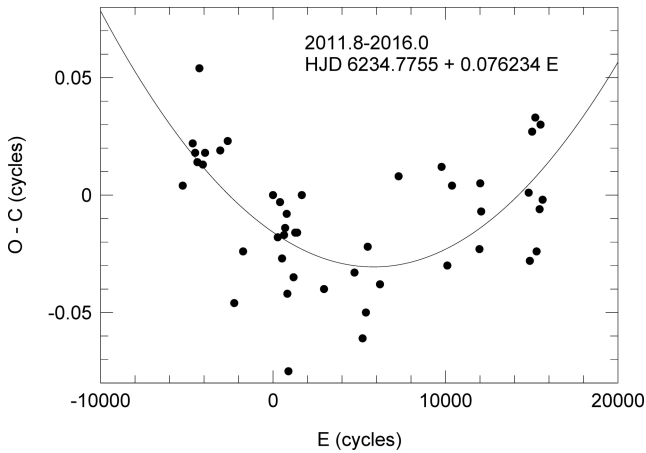


Figure 5. O–C diagram for the timings after the orbital variation reappears. The fitted curve indicates an increasing period, with $P/\dot{P} = 2.4 (4) \times 10^5$ yr.

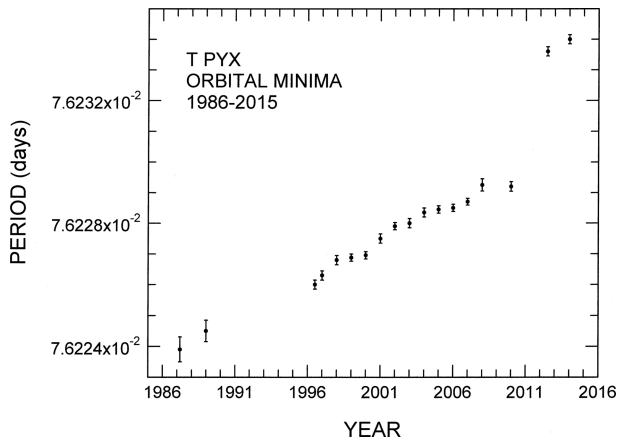


Figure 6. The variation of P_{orb} during 1986–2015. Each point represents a 2-yr running mean. Day zero of the eruption occurred at 2011.4.

are consistent. So, these early points are likely correct, although sceptical readers should feel free to ignore them.

5 ABSOLUTE PHASING OF THE SIGNALS

Despite the large ΔP in eruption, there is no difficulty in measuring the absolute phases across eruption. An O–C diagram of the timings for several years before and after eruption is shown in Fig. 7, and the straight lines indicate linear fits to the timings before and after eruption. The two lines appear to meet at day 120 ± 90 . If the ΔP occurred very rapidly, that event could have occurred at day 0, or as many as 250 d after eruption. A gradual change is also possible, of course.

Perhaps the most interesting aspect of Fig. 7 is not the exact time of the ΔP event, which is unknowable, but rather this: the absolute phasing of minimum light in the orbital cycle appears to be preserved across eruption – at $V = 15.5$, $V = 11$, and possibly even $V = 8$. As demonstrated in Fig. 4, the shape of the light curve is also roughly preserved. Some aspect of binary structure is responsible for the orbital signal, and it seems to be basically independent of luminosity state. In Section 10.1, we will interpret this as a *reflection effect* in the binary, probably augmented by a small partial eclipse.

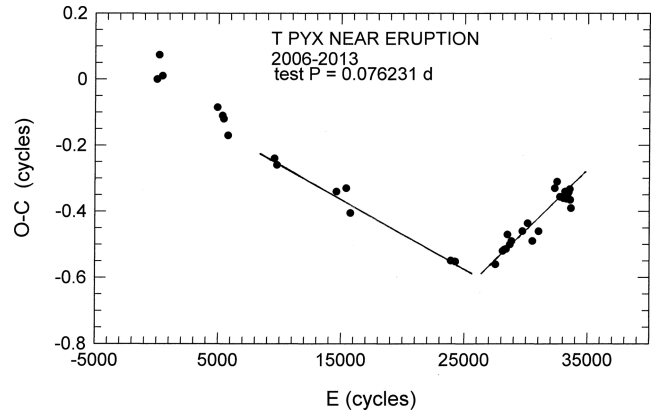


Figure 7. O–C diagram of orbital timings, relative to the test ephemeris in the figure, for several years before and after eruption. The straight lines define an apparent ‘V’ vertex occurring at day 120 ± 90 ; the change in slope indicates a change in period. The main point here is that the signal showed no discontinuity in phase – likely indicating that the periodic signal has the same origin, anchored in binary phase, before, after, and even *during* the eruption.

6 REDDENING, DISTANCE, LUMINOSITY, AND ACCRETION RATE?

In P98, we adopted a distance of 3.5 ± 1.0 kpc and a reddening $E(B-V) = 0.35$. This was emphatically rejected by Gilmozzi & Selvelli (2007), who obtained $E(B-V) = 0.25 \pm 0.02$ from the standard technique of removing the $\lambda 2200$ bump from the UV flux distribution. But as stressed by Fitzpatrick (1999), the scatter in the empirical relationship used to infer reddening from the $\lambda 2200$ bump, even when the fluxes are very accurately known, is at least 20 per cent. For a variable star such as T Pyx, it must be worse, because the two UV spectra (IUE SWP + LWR) were obtained at different times. Godon et al. (2014) revisited this subject, and their fig. 1 shows the UV spectrum combining the *IUE*, *HST*, and *GALEX* spectra. Their fig. 2 shows the result of applying various reddening corrections to that combined spectrum, and the authors settle on $E(B-V) = 0.35$ as the best choice. No error is quoted, but the figure suggests something like $(-0.07, +0.10)$ might be realistic. The diffuse interstellar bands suggest $E(B-V) = 0.44 \pm 0.17$ (Shore et al. 2011). Thus, we consider $E(B-V) = 0.35$ a plausible value. That estimate corresponds to a column density $N_{\text{H}} = 1.9 \times 10^{21} \text{ cm}^{-2}$, according to the correlation of Predehl & Schmitt (1995). This is also consistent with the column densities inferred from X-rays in outburst ($2.0 \times 10^{21} \text{ cm}^{-2}$; Chomiuk et al. 2014; $1.6 \times 10^{21} \text{ cm}^{-2}$, Tofflemire et al. 2013) and HI radio observations on that line of sight ($2.1 \times 10^{21} \text{ cm}^{-2}$; Dickey & Lockman 1990).

The mean magnitudes at ‘quiescence’ are $V = 15.4$, $B-V = 0.07$, $U-B = -0.97$ (Landolt 1970, 1977). Assuming a normal interstellar extinction curve, the de-reddened magnitudes are then $V = 14.3$, $B-V = -0.28$, $U-B = -1.22$. These colours signify a very hot source. They are similar to the colours of a mid-O star, with $T \sim 40\,000$ K and a bolometric correction of ~ 3.5 mag (Flower 1996), and roughly the same for a model DA WD (Koester, Schulz & Weidemann 1979). Sokolowski et al. (2013) measure a distance of 4.8 ± 0.5 kpc from the light echoes seen in the *HST* images (reflecting off ejecta in the nebula). Assuming spherical symmetry and correcting for extinction with the galaxy-averaged $A_V = 3.1 E(B-V)$, the quiescent

T Pyx then has $M_V = +0.9$, $M_{\text{bol}} = -2.6$, or $L = 800 L_{\odot} = 3 \times 10^{36} \text{ erg s}^{-1}$.⁴

Neglecting any contribution from a boundary layer, disc accretion onto a WD of mass near $1 M_{\odot}$ yields a luminosity

$$L = GM_1 \dot{M} / 2R_1 = 3 \times 10^{35} m_1^{1.8} (\dot{M})_{18} \text{ erg s}^{-1}, \quad (3)$$

where M_1 and R_1 are the WD's mass and radius, $(\dot{M})_{18}$ is the accretion rate in units of 10^{18} g s^{-1} , and $m_1 = M_1 / 1 M_{\odot}$ (with $m_1^{1.8}$ incorporating the WD mass–radius relation near $1 M_{\odot}$). Thus, we estimate

$$\dot{M} = 1 \times 10^{19} m_1^{-1.8} \text{ gs}^{-1} = 1.5 \times 10^{-7} m_1^{-1.8} \text{ Myr}^{-1}. \quad (4)$$

7 INTERPRETATION

7.1 Quiescence

In quiescence, T Pyx's secondary transfers matter to the WD – at a very high rate, to account for the high quiescent luminosity and the frequent nova eruptions. If total mass and angular momentum are conserved in this process, then \dot{M} is related to \dot{P} via

$$\dot{M} = q M_1 (\dot{P} / P) / 3(1 - q), \quad (5)$$

where M_1 is the WD mass and $q = M_2 / M_1$. For our measured $\dot{P} = 6 \times 10^{-10}$ (during 1996–2011, when the long baseline confers good accuracy) and the binary parameters formally deduced by UKS ($M_1 = 0.7 M_{\odot}$, $q = 0.2$), this implies $\dot{M} = 1.8 \times 10^{-7} M_{\odot} \text{ yr}^{-1}$. But the line doubling and the photometric modulations (X-ray and optical) are very surprising if the binary inclination is as low as the UKS value ($10 \pm 2^\circ$). Assuming a disc-wind reinterpretation of the velocities, it is possible, though by no means certain, that the *motion* of the emission lines remains a good tracer of the true dynamical motions, although the emission-line *widths* have a completely different origin. In that case, we can still use the UKS result of $v_1 \sin i = 18 \text{ km s}^{-1}$ to infer masses, with a dependence on the unknown inclination.

This constraint is shown in Fig. 8. Of course, binary inclinations much higher than the UKS value drive q much lower; in the vicinity of $i = 50^\circ$ – 60° , the solutions are near $M_1 = 1.1 M_{\odot}$, $M_2 = 0.06 M_{\odot}$. Equation (5) then yields $\dot{M} = 6 \times 10^{-8} M_{\odot} \text{ yr}^{-1}$.

So for a broad range of inclinations, the accretion rate inferred from the luminosity is similar to the mass transfer rate implied by the steady increase in P_{orb} . Both rates are near $10^{-7} M_{\odot} \text{ yr}^{-1}$, if M_1 is near $1 M_{\odot}$. Does such a binary actually make recurrent-nova outbursts? Yes, apparently it does. With these parameters, the models of Yaron et al. (2005, their table 3) erupt every ~ 80 yr, with the time-scale depending sharply on both M_1 and \dot{M} . Thus,

⁴ To sharpen our analysis of the energetics, we should correct for the star's binary inclination. The star has long been regarded as nearly face-on, because the emission lines are relatively narrow and nearly stationary (UKS). But *HST* imaging and radial velocities of the shell ejected in 2011 are more compatible with a *high* binary inclination, and it may be possible to reinterpret the emission lines as arising in an accretion-disc wind, rather than in a rotating disc (Sokoloski et al. 2016). Also, the depth of the binary eclipse in soft X-rays (Tofflemire et al. 2013) is hard to understand with a very low inclination. We consider this to be now an open question. Inclinations above $\sim 70^\circ$ are probably ruled out by the lack of deep eclipses and smallness of the orbital modulation, and inclinations much below 20° have difficulty producing much orbital modulation at all. So, we will take the coward's way out and apply no correction for inclination. In effect, this is equivalent to adopting $i = 50^\circ$ – 60° .

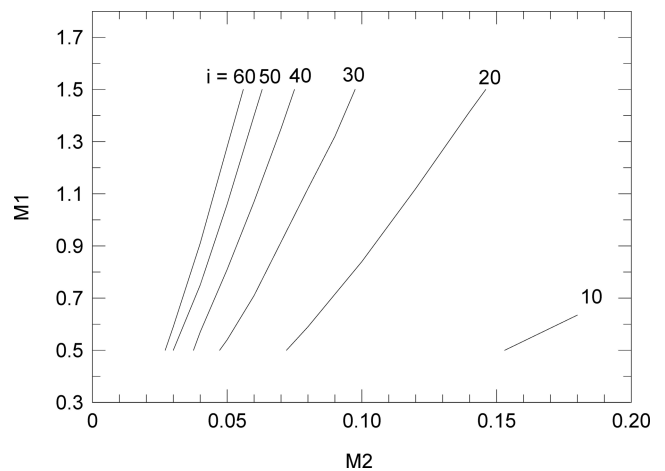


Figure 8. Constraint on the masses, for various choices of binary inclination i . The UKS measurement of $K_1 = v_1 \sin i = 18 \text{ km s}^{-1}$ is used. For the $i > 50^\circ$ inclination (slightly) favoured in this paper, M_2 must be less than $0.06 M_{\odot}$.

our physical parameters in quiescence appear to satisfy⁵ all known constraints.

7.2 Eruption and aftermath

During eruption, mass-loss should increase P_{orb} , and angular momentum loss should decrease it. It is an open question as to which will dominate. But our observations (Figs 6 and 7) show $\Delta P / P = +5.4 \times 10^{-5}$, indicating that mass-loss wins. For the minimum plausible prescription for angular momentum loss (radial ejection from the WD), this implies a mass-loss

$$\Delta M = 3.0 \times 10^{-5} m_1 (1 + q) M. \quad (6)$$

For $m_1 \approx 1$, this represents about 300 yr of accretion, yet only 45 yr elapsed since the 1966 outburst. So the *prima facie* evidence suggests that the nova ejected approximately six times more matter than the WD had accreted.

One can nibble around the edges of this conclusion by revising some numbers (m_1 , q , i , bolometric correction). It is also possible that some of the ejected matter had never been on the WD. But the assumption most susceptible to error is that the nova ejecta carry off very little angular momentum (just the specific angular momentum of the WD). It is easy to imagine ways in which more angular momentum is carried away: from the secondary, from rotation, from frictional losses. But the observed ΔP is large, positive, and undeniable; so each of these would only *raise* ΔM , strengthening the conclusion that the WD erodes (or at least fails to increase its mass significantly; this would be the case if much of the ejected matter never resided on the WD). We note that radio observations (from the free–free emission) also suggest a large ΔM , probably near $10^{-4} M_{\odot}$ (Nelson et al. 2014). Thus, it now seems unlikely that the WD in T Pyx – once considered a fine ancestor for a Type Ia supernova – will ever increase its mass at all, much less reach $1.4 M_{\odot}$.

Caleo & Shore (2015) suggest an alternative hypothesis: that a change in the *eccentricity* of the binary might significantly affect the change in P_{orb} – and therefore that ΔP cannot be used to directly

⁵ Which is not to say that we understand them! So, high a mass-transfer rate from so puny a donor star is unprecedented and mysterious.

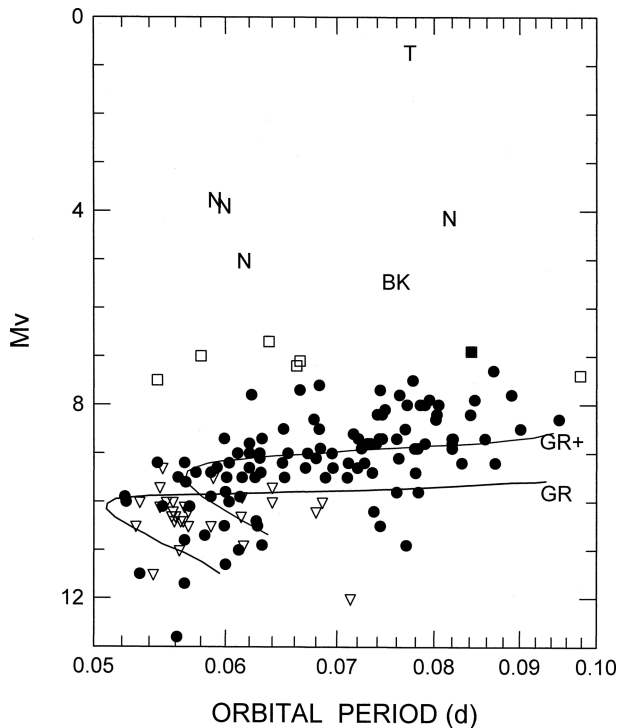


Figure 9. Time-averaged M_V versus P_{orb} for short-period CVs. The average error in $\langle M_V \rangle$, usually dominated by distance uncertainty, is probably near 0.8 mag. This excludes actual nova eruptions, and therefore should predominantly represent *accretion* light. Dots are dwarf novae, triangles are upper limits for dwarf novae (usually because the recurrence time is not known), and the bold boomerang-shaped curve labelled GR is a theoretical main-sequence for CVs. GR+ indicates an ‘enhanced GR’, discussed in the text. Stars labelled N are 20th century novae; ‘T’ is T Pyx, and ‘BK’ is a likely second-century nova. The squares are ER UMa stars – dwarf novae that we interpret as millennia-old classical novae. In our interpretation of the aftermath of classical-nova eruptions, stars drop vertically down from $M_V = -7$, but with ever-increasing slowness, such that $dm/d(\log t) \approx 1$.

infer ΔM . But any change in eccentricity would presumably make only a transient effect on P_{orb} . As the eccentricity relaxed back to zero, P_{orb} should relax back to the value appropriate for $e = 0$. Inspection of Fig. 6 suggests that no such relaxation is occurring. It appears that P_{orb} resumes tracking the normal⁶ \dot{P} of quiescence, as if the eruption never happened. This probably limits the importance of eccentricity change.

8 T Pyx AMONG THE CVs

In the ranks of CVs, T Pyx holds many titles: most luminous, hottest, highest excitation, fastest orbital-period change, most frequently erupting, etc. We have shown, or at least advocated with enthusiasm, that all of these (except perhaps ‘most famous’) can be ascribed to just one property: highest accretion rate.

For stars powered by accretion, time-averaged M_V is a good proxy for \dot{M} , and Fig. 9 shows the empirical data on M_V versus P_{orb} for disc-accreting CVs of short period (< 0.1 d) and ‘known distance’.⁷

⁶ Although the time baseline for this measurement is still rather short, timings through the year 2018 will greatly improve the accuracy of this test.

⁷ Readers will have a variety of opinions concerning what accuracy is required to deserve the adjective ‘known’. More specifically, this is an expanded version of fig. 5 and table 2 of P11, where the distance constraints

Dots and triangles (which are upper limits) show garden-variety dwarf novae, and the superposed bold curve shows the prediction of the standard theory of CV evolution, in which mass transfer is driven by angular momentum loss by gravitational radiation (GR). With a few small but systematic departures, the stars track the theory curve, resembling a boomerang, pretty well. The lighter curve, labelled GR+, shows the corresponding prediction for the slightly enhanced angular momentum loss rate considered by Knigge, Baraffe & Patterson (2011) to improve the fit to the stellar *radii*. Squares denote a small subclass of dwarf novae known as ‘ER UMa stars’. The N symbols indicate 20th-century novae, roughly 50 yr after eruption and often assumed to be in their version of ‘quiescence’. Two stars are shown by name: T Pyx and BK Lyn which is a definite ER UMa star and very likely a 2000-yr-old classical nova (P13).

In the theory peddled by P13, that boomerang-shaped curve⁸ is the main story of CV evolution, but each star experiences classical-nova eruptions that vault the star into the upper regions, where it stays for thousands of years as *something* keeps the accretion rate high. It settles back to near-quiescence after $\sim 50\,000$ yr (see fig. 7 of P13 for a conjecture on the rate of decline). But some stars never get the opportunity to rest after their nova ordeals, because new classical-nova eruptions can interrupt the decline. They may happen with ever-increasing frequency, because eruption frequency scales at least as fast as \dot{M} in the TNR models (see Yaron et al. 2005). Eventually the star can turn into a T Pyx, and then soon die as the secondary is evaporated after ~ 1000 more eruptions ($0.1 M_{\odot}/10^{-4} M_{\odot}$).

This time-scale for dropping to the CV main sequence is discussed by P13, especially in their fig. 11. The key is to recognize that novae seem to fade logarithmically with time, roughly like $dm/d(\log t) \approx 1$. (Not $dm/dt = \text{constant}$, which is often assumed and leads to much shorter estimates for ‘the end of the eruption’.) This is compatible with previous Herculean studies of nova decline rate (Vogt 1990; and especially Duerbeck 1992, who had it all right). But those studies could not reach a strong conclusion because they were hampered by the short baseline available to them (~ 100 yr). This changed with the following recognitions:

- BK Lyn as a likely 2000-yr-old nova;
- very faint pre-eruption magnitudes and limits (Collazzi et al. 2009; Schaefer & Collazzi 2010); and
- the essential difference between the short- P_{orb} novae and their long- P_{orb} cousins that have strong machines (magnetic braking) for generating luminosity unrelated to the nova event (P13).

Another constraint on time-scale comes from consideration of space densities. In our census, there are ~ 5 old novae with an average distance of ~ 2 Kpc, 7 ER UMas with an average distance of 400 pc, and 120 normal dwarf novae with an average distance of 250 pc. For a Galactic distribution with a vertical scaleheight ~ 300 pc, this corresponds to space densities roughly in the ratio 1:100:10000 (where ‘1’ corresponds to $7 \times 10^{-10} \text{ pc}^{-3}$). In our interpretation, this ratio represents the time spent in these various stages. Old novae

are discussed – in general, and also for the individual stars. While some are high-quality distances (e.g. from trigonometric parallax or fitting of stellar-atmosphere models), most are based on standard-candle methods and only good to ~ 40 per cent.

⁸ The empirical version is defined by the dots and triangles. That could perhaps be described as arising from GR plus an additional driver (angular momentum loss, or something tracking or mimicking it) which increases with P_{orb} .

last at least 150 yr (no recent short-period nova has ever become a certified dwarf nova), but probably less than 2000 yr (BK Lyn is transitioning now). So, we speculate that the durations of these states are roughly $10^3:10^5:10^7$ yr. That also agrees at the long end, since it requires ordinary short-period dwarf novae, accreting at $4 \times 10^{-11} M_{\odot} \text{ yr}^{-1}$, to erupt after accumulating $4 \times 10^{-4} M_{\odot}$ – an estimate not far from that of the TNR models ($10^{-4} M_{\odot}$, table 2 of Yaron et al. 2005).

Could the hypothesized slowness of that decline reflect merely the cooling of the WD after outburst? Probably not. After a few years, the stars are dominated specifically by accretion light, as evidenced by all the usual signatures of accretion discs: flickering, broad eclipses, doubled emission lines, power-law flux distribution, positive and negative superhumps, etc. The feeble secondaries in these stars appear to be really transferring matter at unnaturally high rates.

9 THE ORIGIN OF THE MASS TRANSFER

What could maintain these high rates? A plausible mechanism is a wind from the secondary, driven by the intense EUV and supersoft X-ray radiation from the WD. This has been previously discussed by van Teeseling & King (1998) for supersoft binaries, and specifically for T Pyx by Knigge, King & Patterson (2000). EUV and soft X-rays will be absorbed high in the secondary’s atmosphere, and therefore may have no significant direct effect on the star’s structure, but all that energy can be very effective in driving a wind. Some of the wind escapes uneventfully, and some is captured by the WD. If the WD mass and accretion rate are high enough, nuclear burning occurs and we see a WD shining with $L_{\text{bol}} = 10^{36}\text{--}10^{37}$ erg s^{-1} , $T = 500\,000$ K (a ‘supersoft binary’). If the WD mass and/or accretion rate are somewhat lower, then accretion probably dominates the energy budget and we see a source of lower luminosity and temperature – until years later, when the accumulated fuel burns explosively.

This is different from the popular model for supersoft sources, in which thermal-time-scale mass transfer occurs from a 1–2 M_{\odot} secondary (van den Heuvel et al. 1992). As pointed out by Oliveira & Steiner (2007, hereafter OS), the mass ratio $q = M_2/M_1$ can in principle be tested by observing the rate of orbital period change. For conservative mass transfer, $\dot{P} < 0$ implies $q > 1$, and $\dot{P} > 0$ implies $q < 1$ (see equation 5). Evolution changes both q and P rapidly, and there is also a Roche-lobe-filling constraint. OS’s fig. 1 shows the expected variation of P/\dot{P} in the two basic models, and demonstrates that the sign of P/\dot{P} discriminates between them. In particular, OS argues that the observed period increase in CAL 87 supports the theory of wind-driven mass transfer, even for that famous star – the original charter member of the supersoft binary club. This also agrees with the masses obtained from radial velocities by Hutchings et al. (1998).

For most stars classified as supersoft binaries, the \dot{P} values are unknown. Almost all are in other galaxies, and hence not visited sufficiently often by telescopes to measure \dot{P} . Fully credentialed Milky Way supersofts are far less numerous, because of soft X-ray absorption in the Galactic plane. But in an important paper, Steiner & Diaz (1998) pointed out that the Milky Way contains a class of stars – which they termed ‘V Sge stars’, a name that has stuck – which resemble the supersofts pretty thoroughly, except for the defining property of intense soft X-ray flux. P98 also advocated the inclusion of such stars, especially the two described in that paper (V Sge and T Pyx). All the proposed V Sge members are broadly similar to the supersofts in luminosity, accretion rate, spectrum

and excitation, orbital period, orbital light curves, and they have measured \dot{P} s which show that they, like the supersofts, are in short-lived states. It would be quite advantageous if we can study our specimens at 11th magnitude!

Like CAL 87 and most of the V Sge stars (except V Sge itself), T Pyx has a large positive \dot{P} , as expected for radiation-driven winds from a low-mass secondary.

10 ORBITAL PHASE: WHAT DOES IT MEAN?

10.1 Radial-velocity and light variations

The UKS spectroscopic study found that the emission-line source reached superior conjunction (red-to-blue crossing) at the time of minimum light. That would be natural if minimum light arises from an *eclipse* of the accretion disc by the secondary. Indeed, a small eclipse may be present, but the orbital wave varies smoothly around the orbit, so the main effect is probably different.

The same phase relation between light and velocities is produced by a reflection effect, with the secondary heated by the intense emission from the WD and its vicinity. But if that radiation is isotropic and direct, then at most ~ 1 per cent can reach the small secondary, and possibly none at all from the disc that radiates perpendicular to the orbital plane. The *disc rim and hot spot* (where the mass-transfer stream strikes the disc) are more promising. At a high accretion rate, the disc is likely to be large (minimizing the phase offset between the spot and the secondary) and possessing a relatively high rim. Even with no help from the central object, a classical disc should be concave, with a vertical height scaling as $r^{9/8}$ (Pringle & Rees 1972). This gives a favourable geometry for heating at the rim, reprocessing radiation from the central object. Add a slight bulge on the rim, presumably from stream impact, and incident radiation from disc centre can puff it up further and create the substantial asymmetry on the disc that is needed to fit this hypothesis to the light curves.

This is the essence of the model that has been used with success to fit the optical light curve of the supersoft binary CAL 87 (Meyer-Hofmeister, Schandl & Meyer 1997; Schandl, Meyer-Hofmeister & Meyer 1997; see also Armitage & Livio 1998; Spruit & Rutten 1998). As remarked in P98 (see figs 3, 6, and 10 of that paper), the CAL 87 optical light curve bears close resemblance to that of T Pyx, and is nearly indistinguishable from that of V Sge. This appears to be substantially true for the radial velocities as well. The periodic dips in CAL 87 occur at the same time the emission-line source reaches superior conjunction (Hutchings et al. 1998; see their table 3 and fig. 9). It is no surprise in CAL 87, because that star shows optical and X-ray eclipses, with an orbital inclination estimated as $\sim 82^\circ$ (Ribeiro, Lopes de Oliveira & Borges 2014). In V Sge, the He II emission line reaches superior conjunction at eclipse phase 0.93 ± 0.05 (Diaz 1999). V Sge’s eclipse depths vary greatly but predictably, with minimum depth when the star is in one of its bright states. The orbital inclination is estimated as $\sim 70^\circ$ (Smak, Belczynski & Zola 2001), permitting a true eclipse, so the observed eclipse ought to coincide (and does) with the time of conjunction.

When the orbital dip does not have the depth and overall signature of a true eclipse arising from high orbital inclination, it is harder to interpret. But we note that the light and radial-velocity variations of the supersoft binary SMC 13 = 1E 0035.4–7230 which at $P_{\text{orb}} = 4.1$ h is T Pyx’s closest known cousin among the acknowledged supersofts, also follow this pattern – with red-to-blue crossing at photometric phase 0.00 ± 0.03 (Crampton et al. 1997). The orbital

wave in this star is approximately sinusoidal, with a full amplitude of 0.24 mag. Radial velocities appear to track the WD in all four stars, with the photometric wave plausibly attributed to a reflection effect, and the difference in light curves (amplitude and symmetry) plausibly attributed to the accident of orbital inclination.

10.2 The orbital wave in X-rays

The soft X-rays come from a compact source, so any reasonable person would expect their orbital light curves to depend strongly on i : deep, short, and sharp eclipses for an edge-on binary, and very flat for binaries of lower i . But observations contradict this. Tofflemire et al. (2013) present the light curve for the supersoft source in T Pyx, which is a smooth sinusoid with minimum phased with the optical minimum. Ribeiro et al. (2014, see also Schmidtke et al. 1993) present the light curve of CAL 87 that also shows a smooth variation, plus at most a *partial* eclipse near optical minimum. These light curves imply that the X-ray source is quite large – an X-ray ‘corona’ that presumably scatters X-rays coming from the WD.

10.3 The secondary

With all this talk of a raised disc rim and only ~ 1 per cent of the WD’s luminosity is able to reach the secondary even on a fully transparent line of sight, how does the secondary manage to be heated, as we have alleged in Section 9? Heating of the secondary is the linchpin of the whole machine. We do not fully, or maybe even partially, understand this. But the X-ray corona provides a promising channel. To satisfy the CAL 87 X-ray light curve, it should be comparable to the entire disc in size, and can scatter X-rays towards the donor star with no great intervening opacity.

Also, the two ΔP events in T Pyx – the impulsive one in eruption, and the steady one in quiescence – imply the possibility of asynchronous rotation. Tides synchronize a binary quickly, but not as quickly as the observed ΔP events may *unsynchronize* this particular binary. There is a lot of energy in an M star rotating with $P = 1.8$ h. Tides will rapidly couple the outside of the star to the orbit, and less rapidly the inside. The resultant shear could conceivably add heat to the star – throughout, not just in its upper atmosphere.

The constraint of very low donor-star mass ($M_2 < 0.06 M_\odot$), plus the observation of a steady P_{orb} increase, suggest that T Pyx is a ‘period bouncer’ – that much-discussed final phase of CV evolution. But all previous discussions (e.g. Kolb & Baraffe 1999; P11) have assumed that it occurs at *low* luminosity, totally unlike T Pyx. Still, the essence of period bounce is that an evolutionary process is inflicted on the secondary faster than its thermal time-scale. With a high luminosity, a puny secondary, and the likelihood of high heating, that appears to be very probable for T Pyx. This appears to be a separate channel of cataclysmic-variable demise, which we are only now learning about, because this phase is so very rapid.

11 WHITHER T Pyx?

We have now tracked the P_{orb} evolution through 30 yr – just about the average interval between eruptions. The observations include an eruption, and the six known eruptions are pretty close counterparts, at least in their light curves. So, with a little nip from Ockham’s Razor, but without proof of course, it seems reasonable to consider the possibility that this evolution will continue: with P_{orb} ever increasing, each nova event carrying off $\sim 10^{-4} M_\odot$, and progressively

whittling down the secondary to smaller mass. The future would then hold ~ 1000 ($=10^{-1} M_\odot/10^{-4} M_\odot$) more eruptions, and then the secondary evaporates.

We have always wondered why T Pyx is unique. This scenario offers a candidate explanation: because it is dying – annihilating its secondary in a paroxysm of repeated nova events, and lasting only $\sim 20\,000$ more years at the current rate. Some of the population statistics of cataclysmic variables (total space densities, ratio of long-period to short-period CVs) would make more sense if there were a way to kill off short-period CVs, thereby preventing them from swamping the local census. This is ‘the problem of the dead novae’, which has been with us for a long time (Patterson 1984, sections VIIc and VIIIe; Patterson 1998, sections 6.3 and 6.4). It could also solve the problem of the missing period bouncers (the puzzling rarity of stars on the lower – largely invisible – part of the boomerang in Fig. 8). T Pyx may offer us an embarrassingly gaudy but practical way to solve these problems.

12 SUMMARY

(1) We provide a full report of the CBA campaign during 1996–2016, following our previous accounts (P98, P14, and the ephemeris in UKS). We acquired ~ 2000 h of time-series photometry before, during, and after outburst.

(2) Except for ~ 100 d after the rapid rise to outburst, the star always shows a distinct 0.07623 d photometric wave, with a full amplitude smoothly varying from 0.004 mag (at $V = 11$) to 0.08 mag (at $V = 15.7$). The waveform is nearly sinusoidal, but small and variable dips near the phase of maximum light leads us to adopt *minimum* light as the best fiducial mark of phase. We refer to the signal as ‘orbital’, for several reasons.

(a) No other period is found in the best-quality data sets – those with densely clustered time series and of adequate length. Binary stars may or may not have other periods, but they definitely need to have an orbital period.

(b) The period is always present, with the same phase and amplitude (at quiescence).

(c) The P98 ephemeris successfully predicts the minima for many years ahead.

(d) The exact ephemeris agrees with the velocities from the UKS spectroscopic study.

(e) The photometric and spectroscopic phases agree, for an arguably natural choice of interpretation, where minimum light coincides with superior conjunction of the emission-line source.

(3) During quiescence (1996–2011, and probably 1986–2011), the period increased smoothly on a time-scale $P/\dot{P} = 3 \times 10^5$ yr. We interpret this as due to mass transfer at a rate near $10^{-7} M_\odot \text{ yr}^{-1}$. This also agrees with the accretion rate required to power the luminosity.

(4) Somewhere near day 120 ± 100 days after the initial rise to outburst, the orbital period changed to 0.0762336 d – an increase of 0.0054(5) per cent over the value before outburst. This change, shown in Figs 6 and 7, took place over an interval of less than 1.5 yr, and was probably caused by the ejection of at least $3 \times 10^{-5} M_\odot$. This exceeds the mass transfer during the previous 45 yr, suggesting that the WD mass is probably eroding. It is hard to grow WD mass in a system that has nova outbursts!

(5) During 2012–2016, the orbital period resumed its increase, at a rate similar to that seen during the 25 yr prior to eruption. This tends to support the idea that the dominant origins of the ΔP effects are pretty straightforward: mass transfer in quiescence, mass-loss in outburst.

(6) The soft X-ray light curve (Tofflemire et al. 2013) shows a large orbital dip in phase with the dip in optical light. This is plausible if the binary inclination is somewhat high ($>50^\circ$), and this is also suggested by the *HST* imaging and radial velocities of the ejected shell. A re-analysis of the UKS radial velocities at quiescence suggests that M_2 may not exceed $0.06 M_\odot$ (Fig. 8).

(7) The M_V - P_{orb} relation for short-period CVs that are non-magnetic and powered by accretion is shown in Fig. 9. As is well known, the novae are around $M_V = 4$ and the dwarf novae are mostly around $(M_V) = 9-10$ – with the recently discovered ER UMa class around $(M_V) = 7$. We propose that every star’s location above the ‘CV main sequence’ (the boomerang) reflects mainly time since the last nova eruption. The total time to return to the boomerang is probably 10 000–100 000 yr. Enhanced mass transfer for so long an interval produces a few strangely but briefly bright stars (old novae and ER UMas), but also can be significant in speeding up every star’s long-term evolution. If \dot{M} is high enough, it can ignite new nova eruptions before the star can rest from its last one. We interpret T Pyx as an extreme example of this (hypothetical) process.

(8) The linchpin of this scenario is the secondary star that must transfer matter at unnaturally high rates. This probably occurs through a radiation-driven wind, as is thought to operate for several (most?) of the supersoft binaries.

(9) The orbital light curve is unusual among accretion-powered CVs, but very similar to that of V Sge stars and several supersoft binaries. In all four stars we consider, the velocities show that the emission-line source (disc) is at superior conjunction at the time of minimum light. Both a reflection effect and a geometrical eclipse are consistent with this phase, and both are likely significant.

(10) The estimated space density of active CVs is $\sim 10^{-5} \text{ pc}^{-3}$, and most of these are short- P_{orb} stars (Patterson 1998). With a characteristic scaleheight of 300 pc, there should be about 300 000 CVs out to the distance of T Pyx. Any of these stars with the properties of T Pyx would be impossible to hide; some would actually be naked-eye stars (briefly). But we only know of one. We interpret this to mean that it is in a very unusual phase of its life, maybe the last phase, in which it evaporates its donor star after ~ 1000 more eruptions. This fate could await other short-period novae, once their secondaries become sufficiently light and less able to cope with the damage from nova events. This could be a major channel by which classical novae – and therefore all CVs – are removed from the population.

(11) In our effort to understand this mysterious star, we have placed a lot of emphasis on light curves and periods. This seems to have been productive, but admittedly, ‘when you have a hammer, everything looks like a nail’ (Maslow 1966). We now wait for others, wielding different hammers, to move the story beyond the level of comprehension we have staggered into.

ACKNOWLEDGEMENTS

The 20-yr path to this paper’s emergence has been made possible by a medley of grants from the National Science Foundation (most recently AST12–11129), NASA, and the Mount Cuba Astronomical Foundation. Discussions with Christian Knigge, Koji Mukai, Jen Sokoloski, and Brad Schaefer have sharpened our ideas about novae, and occasionally stymied our speculations with uncomfortable facts. We apologize for the irregular way (rumours, private communications) the results have been leaking out – a poor model for scientific work. We will do better next time!

REFERENCES

- Barrera L. H., Vogt N., 1989, *Rev. Mex. Astron. Astrofis.*, 19, 99
 Caleo A., Shore S. N., 2015, *MNRAS*, 449, 25
 Chomiuk L. et al., 2014, *ApJ*, 788, 130
 Collazzi A. C. et al., 2009, *AJ*, 138, 1846
 Crampton D., Hutchings J. B., Cowley A. P., Schmidtke P. C., 1997, *ApJ*, 489, 903
 Diaz M. P., 1999, *PASP*, 111, 76
 Dickey J. M., Lockman F. J., 1990, *ARA&A*, 28, 215
 Duerbeck H. W., 1992, *MNRAS*, 258, 629
 Fitzpatrick E. L., 1999, *PASP*, 111, 63
 Flower P. J., 1996, *ApJ*, 469, 355
 Gilmozzi R., Selvelli P., 2007, *A&A*, 461, 593
 Godon P. et al., 2014, *ApJ*, 784, L33
 Hutchings J. B., Crampton D., Cowley A. P., Schmidtke P. C., 1998, *ApJ*, 502, 408
 Knigge C., Baraffe I., Patterson J., 2011, *ApJS*, 194, 78
 Knigge C., King A. R., Patterson J., 2000, *A&A*, 364, L75
 Koester D., Schulz H., Weidemann V., 1979, *A&A*, 76, 262
 Kolb U., Baraffe I., 1999, *MNRAS*, 309, 1034
 Landolt A., 1970, *PASP*, 82, 86
 Landolt A., 1977, *PASP*, 89, 574
 Livio M., 1991, *ApJ*, 369, L5
 Maslow A. H., 1966, *The Psychology of Science: A Reconnaissance*. Harper & Row, New York
 Meyer-Hofmeister E., Schandl S., Meyer F., 1997, *A&A*, 321, 245
 Nelson T. et al., 2014, *ApJ*, 785, 78
 Oliveira A. S., Steiner J. E., 2007, *A&A*, 472, L21 (OS)
 Patterson J., 1984, *ApJS*, 54, 443
 Patterson J., 1998, *PASP*, 110, 1132
 Patterson J., Raymond J. C., 1985, *ApJ*, 292, 550
 Patterson J. et al., 1998, *PASP*, 110, 380 (P98)
 Patterson J. et al., 2013, *MNRAS*, 434, 1902
 Predehl P., Schmitt J. H. M. M., 1995, *A&A*, 293, 889
 Pringle J. E., Rees M. J., 1972, *A&A*, 21, 1
 Ribeiro T., Lopes de Oliveira R., Borges B. W., 2014, *ApJ*, 792, 20
 Schaefer B. E., 1990, *ApJ*, 355, L39
 Schaefer B. E., Collazzi A. C., 2010, *AJ*, 139, 1831
 Schaefer B. E., Landolt A. U., Vogt N., Buckley D., Warner B., Walker A. R., Bond H. E., 1992, *ApJS*, 81, 321 (S92)
 Schaefer B. E., Pagnotta A., Shara M. M., 2010, *ApJ*, 708, 381 (SPS)
 Schaefer B. E. et al., 2013, *ApJ*, 773, 55 (S13)
 Schandl S., Meyer-Hofmeister E., Meyer F., 1997, *A&A*, 318, 73
 Schmidtke P. C., McGrath T. K., Cowley A. P., Frattare L. M., 1993, *PASP*, 105, 863
 Selvelli P., Cassatella A., Gilmozzi R., Gonzalez-Riestra R., 2008, *A&A*, 492, 787
 Shore S. et al., 2013, *A&A*, 549, 140
 Shore S. N., Augusteijn T., Ederoclite A., Uthas H., 2011, *Astron. Telegram*, 3306
 Skillman D. R., Patterson J., 1993, *ApJ*, 417, 298
 Smak J. I., Belczynski K., Zola S., 2001, *Acta Astron.*, 51, 117
 Sokoloski J. L., Crotts A. P. S., Lawrence S., Uthas H., 2013, 770, L33
 Spruit H. C., Rutten R. G. M., 1998, *MNRAS*, 299, 768
 Steiner J. E., Diaz M. P., 1998, *PASP*, 110, 276
 Tofflemire B. M. et al., 2013, *ApJ*, 779, 22
 Uthas H., Knigge C., Steeghs D., 2010, *MNRAS*, 409, 237 (UKS)
 Van den Heuvel E. P. J., Bhattacharya D., Nomoto K., Rappaport S. A., 1992, *A&A*, 262, 97
 Van Teeseling A., King A. R., 1998, *A&A*, 338, 957
 Vogt N., 1990, *ApJ*, 356, 609
 Yaron O., Prialnik D., Shara M. M., Kovetz A., 2005, *ApJ*, 623, 398

This paper has been typeset from a $\text{\TeX}/\text{\LaTeX}$ file prepared by the author.